Wrench Capability Analysis of Aerial Cable Towed Systems

Julian Benedict Czapalay Erskine, Abdelhamid Chriette, Stéphane Caro

the ASME 2018 International Design Engineering Technical Conferences &
Computers and Information in Engineering Conference
IDETC/CIE 2018
August 26-292018Quebec CityCanada

DETC2018-85378

WRENCH CAPABILITY ANALYSIS OF AERIAL CABLE TOWED SYSTEMS

Julian Erskine[1], **Abdelhamid Chriette**[1,2], **Stéphane Caro**[2,3*]
[1] École Centrale de Nantes, Nantes, 44321 France
[2] Laboratoire des Sciences du Numérique de Nantes (LS2N), UMR CNRS 6004, Nantes, 44300, France
[3] Centre National de la Recherche Scientifique (CNRS), Nantes, 44321, France
Emails: julian-benedict-czapalay.erskine@eleves.ec-nantes.fr
abdelhamid.chriette@ls2n.fr, stephane.caro@ls2n.fr

ABSTRACT

Aerial cable towed systems (ACTSs) can be created by joining unmanned aerial vehicles (UAVs) to a payload to extend the capabilities of the system beyond those of an individual UAV. This paper describes a systematic method of evaluating the available wrench set and the robustness of equilibrium of ACTSs by adapting wrench analysis techniques used in cable-driven parallel robots to account for the constraints of quadrotor actuation. Case studies are provided to demonstrate the analysis of different classes of ACTSs, as a means of evaluating the design and operating configurations.

Keywords*: Quadrotor, Cable Robot, Wrench Feasibility, Capacity Margin*

1 INTRODUCTION

Aerial cable towed systems (ACTSs) are a class of aerial manipulator that is gaining interest as a means of payload transportation and manipulation. Currently most ACTSs are slung loads from helicopters for the purpose of military or civilian logistics, but the recent increase in the commercialization of unmanned aerial vehicles (UAVs) due to improved onboard sensing and computation, and higher energy density batteries has opened the commercial possibility of using many small UAVs to collaborate towards single tasks [1, 2, 3]. ACTSs are composed of aerial vehicles connected to either a rigid body payload or to a point mass through cables. Systems of multiple UAVs give greater versatility in the control of the payload and expand the available task set of the system, as well as delivering an attractive degree of modularity. Many types of UAVs exist, however much of the current research is focused on quadrotors due to their high payload to weight ratio, versatile control, and simple mechanical design [4].

Much of the current research into ACTSs is focused on designing trajectory tracking controllers for the suspended body. In [5], differential flatness is used to generate feasible trajectories for the system. The authors of [6] use control methods adapted from cable-driven parallel robots (CDPRs) to ensure stability and trajectory convergence, while in [7], a linear quadratic regulator is used to control the robot. In [8], a novel ACTS is presented and uses RRT graphs to determine feasible payload trajectories. In all these works the wrench feasibility and stability of the ACTS is considered, but there is no systematic quantification of the degree of wrench feasibility in task space.

There are strong similarities between ACTSs and CDPRs, indeed an ACTS can be considered as a CDPR with moving pulley anchor points. Wrench capabilities have been an important topic of research for CDPRs, playing an important role in their design, workspace analysis, and trajectory generation [9, 10, 11, 12]. The link between CDPRs and ACTSs has been investigated by using tension distribution algorithms for the purposes of control and stability [6, 13]. In [14], the degree of wrench inclusion is used as a performance index for CDPRs. Despite the similitudes of the two types of systems, there are differences in the modelling of the available wrench set due to

*Address all correspondence to this author.

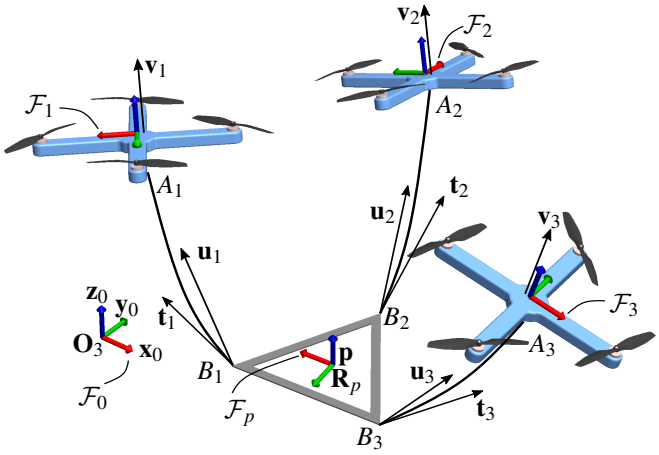

FIGURE 1: PARAMETERIZATION OF AN AERIAL CABLE TOWED SYSTEM COMPOSED OF THREE QUADROTORS, THREE CABLES, AND A RIGID PLATFORM

the actuation limits of quadrotors. The purpose of this paper is therefore to develop a broadly applicable means of evaluating the available wrench set of ACTSs, with possible applications in design, motion planning, and for evaluating the robustness of equilibrium. In this paper, only quasi-static operations are considered, however the methods shown here may later be adapted to dynamic flight.

Section 2 of this paper describes the parameterization of ACTSs. In section 3, the equilibrium conditions of the platform and quadrotors are formalized. The methodology used for calculating the available wrench set of the ACTS is shown in section 4 for a simple planar system. Several case studies are presented in section 5, showing the application for more complex planar and spatial systems. The paper finishes with the conclusion, list of nomenclature, and an appendix of mathematical proofs.

2 GEOMETRIC PARAMETERIZATION

There are different types of ACTSs so a parameterization allowing for design variability is important. From a practical perspective, it is assumed that the pose of the bodies are known with respect to an inertial frame $\mathcal{F}_0$ (many experiments use multi-view visual motion capture). The platform frame $\mathcal{F}_p$ is placed at the center of mass and inertia of the payload. Its position vector $\mathbf{p}$ is expressed in $\mathcal{F}_0$, and in the case of rigid body loads, the orientation is expressed by the rotation matrix $\mathbf{R}_p$.

The ACTS is taken to have n quadrotors where the i^{th} quadrotor has frame $\mathcal{F}_i$ at the center of mass $\mathbf{x}_i$ of the quadrotor, and has a rotation matrix $\mathbf{R}_i$ defined with respect to $\mathcal{F}_0$. The point where the j^{th} cable connects to the moving platform is called B_j, and is expressed in $\mathcal{F}_0$. The cartesian coordinate vector B_j is defined in $\mathcal{F}_p$ as $\mathbf{b}_j$. The j^{th} cable connects the payload to the i^{th} quadrotor and is attached to that quadrotor at point A_i in space

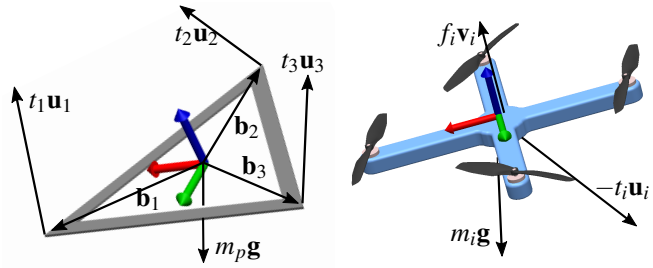

FIGURE 2: FREE BODY DIAGRAMS OF THE MOVING PLATFORM AND THE i^{th} QUADROTOR

(here assumed congruent with $\mathbf{x}_i$), and the cable has a known length l_j. The configuration of the ACTS is described by the set of cable vectors $\mathbf{u}_{1\ldots,m}$, with $\mathbf{u}_i$ being the unit vector pointing from point B_i to point A_i, $i = 1,\ldots,m$. As a function of measured states, the cable vector $\mathbf{u}_i$ is given by Eq.(1).

$$l_i\mathbf{u}_i = \mathbf{x}_i - \mathbf{p} - \mathbf{R}_p\mathbf{b}_i \tag{1}$$

3 STATIC EQUILIBRIUM CONDITIONS OF ACTS

This paper describes the available wrench set of ACTSs in a quasi-static equilibrium situation. It is considered that an external wrench $\mathbf{w}_e = [\mathbf{f}_e^T, \mathbf{m}_e^T]^T$ expressed in $\mathcal{F}_0$ acts on the platform. The equilibrium equations acting on the platform and on the quadrotors are expressed separately in determining the system equilibrium, effectively dividing the systems into three components; the quadrotors, the platform, and the cables linking the two together.

Platform

Assumption 1: Cables are considered to be massless and inelastic. This means that the cables can be considered as straight lines, and as such the i^{th} cable tension vector can be approximated as $\mathbf{t}_i = t_i\mathbf{u}_i$.

The wrenches on the payload are generated through the sum of m tension vectors and their corresponding moments, along with gravity acting at the center of mass. There are therefore $m+1$ constraining wrenches on the payload. In cases where the payload is considered a point mass, the moments generated by the cables are disregarded. As a result, the static equilibrium equations of the platform expressed in frame $\mathcal{F}_0$ are expressed as follows:

$$m_p\mathbf{g} + \sum_{j=1}^{m}(t_j\mathbf{u}_j) + \mathbf{f}_e = \mathbf{0}_3 \tag{2}$$

$$\sum_{j=1}^{m}(\mathbf{R}_p\mathbf{b}_j \times t_j\mathbf{u}_j) + \mathbf{m}_e = \mathbf{0}_3 \tag{3}$$

where m_p is the mass of the platform, $\mathbf{g}$ is the gravitational vec-

tor $[0,0,-9.81]^T ms^{-2}$, and m is the total number of cables connected to the platform.

Quadrotors

The actuation wrench of the i^{th} quadrotor is expressed in $\mathcal{F}_i$ as ${}^i\mathbf{w}_i = [{}^i\mathbf{f}_i^T, {}^i\mathbf{m}_i^T]^T$, where ${}^i\mathbf{f}_i$ is the thrust vector $[0,0,f_i]$ and ${}^i\mathbf{m}_i$ is the moment vector $[m_{i,x}, m_{i,y}, m_{i,z}]$ [4]. The components of ${}^i\mathbf{w}_i$ take the form:

$$f_i = \sum_{i=1}^{i=4} C_F \omega_i^2 \tag{4a}$$

$$m_{x,i} = C_F r_i \left(\omega_1^2 - \omega_3^2\right) \tag{4b}$$

$$m_{y,i} = C_F r_i \left(\omega_2^2 - \omega_4^2\right) \tag{4c}$$

$$m_{z,i} = C_M \left(\omega_1^2 - \omega_2^2 + \omega_3^2 - \omega_4^2\right) \tag{4d}$$

where ω_i is the anguar velocity of the i^{th} propellor, r_i is the distance from the center of the i^{th} propellor to the quadrotor's center of mass, and C_F and C_M are the coefficients of thrust and drag of the propellors, respectively. It can be seen that a quadrotor exerts a thrust normal to the plane containing its rotors, and three independent moments about its center of inertia. This results in four degrees of actuation controlling the orientation of the unit vector $\mathbf{v}_i = \mathbf{R}_i[0,0,1]^T$, and the magnitude of the thrust f_i along $\mathbf{v}_i$.

Assumption 2: Cables pass through the center of mass of the quadrotor to which they are attached. This allows the assumption that in static equilibrium, f_i is the only non-null component of ${}^i\mathbf{w}_i$.

The static equilibrium equations of the i^{th} quadrotor expressed in $\mathcal{F}_0$ are written as:

$$f_i\mathbf{v}_i + m_i\mathbf{g} - \sum_{j=1}^{k} t_j\mathbf{u}_j = \mathbf{0}_3 \tag{5}$$

$${}^i\mathbf{m}_i = \mathbf{0}_3 \tag{6}$$

where k is the number of cables connected to the i^{th} quadrotor and m_i is the mass of the i^{th} quadrotor.

4 AVAILABLE WRENCH SET

With the ultimate goal of determining the available wrench set of ACTSs, the mapping of cable tension space used with CDPRs [14,15] has been adapted to take into account quadrotor constraints. The main difference between the CDPR and the ACTS available wrench sets is that CDPRs have a constant available tension set regardless of the state of the robot, so for any configuration of the CDPR the minimum and maximum available cable tensions are constant. Because a component of the actuation of the quadrotor is required to keep itself in the air, different

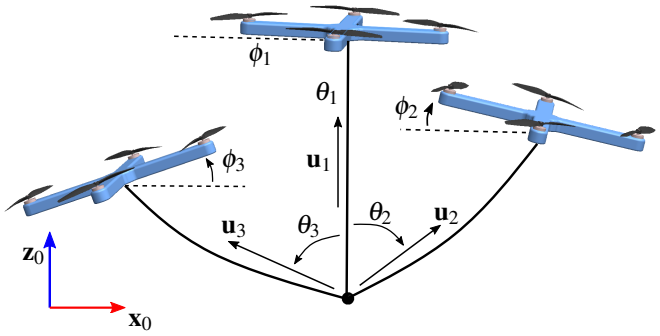

FIGURE 3: ACTS WITH 3 QUADROTORS, 3 CABLES, AND A POINT-MASS PLATFORM

configurations will result in variable tension spans achievable by the ACTS, in turn affecting the set of available wrenches in task space. To this end, an extra mapping step is proposed to go from the thrust space of the quadrotors to the tension space of the cable system.

During the explanation of the available wrench set calculations, an example of a planar ACTS (Figure 3) composed of three quadrotors with a single cable each attached to a point mass will be used. It has the configuration $[\theta_1, \theta_2, \theta_3] = [0, \frac{\pi}{4}, -\frac{7\pi}{18}] rad$, and a payload mass of $m_p = 4kg$. The quadrotors used have a mass of $m_i = 0.8kg$ and maximum thrust of $\bar{f}_i = 32N$. In a general case, there are n quadrotors, m cables, and a task space of dimension d, satisfying the following requirements:

$$1 \leq d \leq 6 \quad \text{and} \quad d \leq m \quad \text{and} \quad n \leq m$$

Thrust Space

As the i^{th} cable of this ACTS connects with the i^{th} quadrotor at $\mathbf{x}_i$ and can only transmit internal tensions, the thrust f_i is the only component of ${}^i\mathbf{w}_i$ that gets transmitted to the payload. Quadrotor i's thrust f_i is bounded by the minimum thrust $\underline{f}_i$ required for hovering, and the maximum thrust $\bar{f}_i$ that the quadrotor can generate. In this paper, an assumption is made that the tension force exerted by the cable on the quadrotor always has a positive projection along $\mathbf{g}$ (each quadrotor is above its attachment point(s)), allowing the minimum thrust to be determined by Eq. (7), as a function of the minimum allowable cable tension $\underline{t}$, where $\underline{t}_i > 0$.

$$\underline{f}_i = \left\| \sum_{j=1}^{k} \underline{t}_j\mathbf{u}_j - m_i\mathbf{g} \right\| \tag{7}$$

The upper bounds of the thrust space are simply the maximum thrust the quadrotors are able to generate. In the planar case study with three quadrotors, the thrust space is a 3-orthotope (Figure

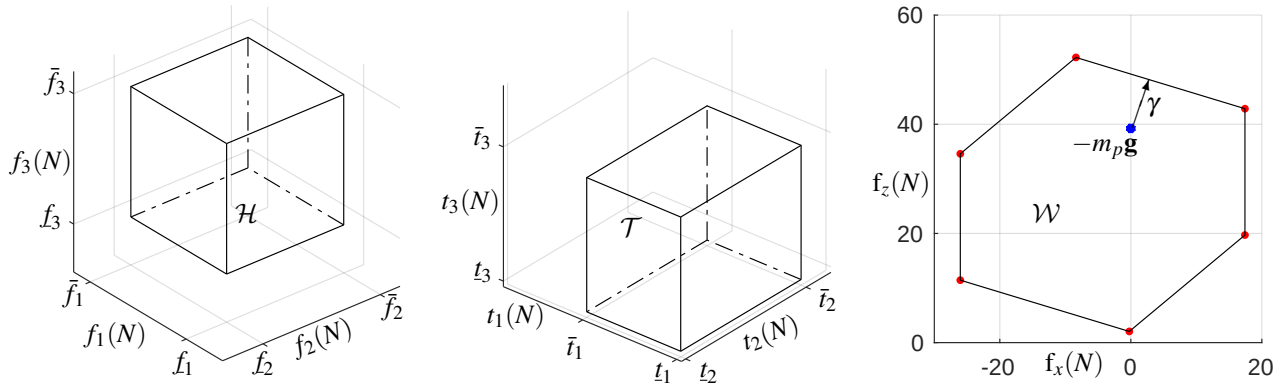

A) THRUST SPACE B) TENSION SPACE C) WRENCH SPACE

FIGURE 4: THRUST, TENSION, AND WRENCH SPACES OF PLANAR ACTS WITH 3 QUADROTORS AND 3 CABLES

4a). The thrust space $\mathcal{H}$ can be generalized for an arbitrary ACTS as the n-dimensional set of independently achievable quadrotor thrusts, forming an n-orthotope:

$$\mathcal{H} = \left\{\mathbf{f} \in \mathbb{R}^n : \underline{\mathbf{f}} \leq \mathbf{f} \leq \bar{\mathbf{f}}\right\} \tag{8}$$

where $\mathbf{f} = [f_1, \ldots, f_n]^T$.

Tension Space

Assumption 3: Cables tensions remain always positive

Tension space is the set of tensions that the quadrotors are able to exert on the cables. Each cable j has tension t_j such that $0 < \underline{t}_j \leq t_j \leq \bar{t}_j$. The minimum tension is a chosen such that there will not be excessive sag in the cable, and the maximum tension is the maximum force the quadrotor can exert on the cable (assumed to be less than the cable's safe operating tension). Accordingly, the tension space can be generalized as:

$$\mathcal{T} = \{\mathbf{t} \in \mathbb{R}^m : \underline{\mathbf{t}} \leq \mathbf{t} \leq \bar{\mathbf{t}}\} \tag{9}$$

where $\mathbf{t} = [t_1, \ldots, t_m]^T$. As each cable is supported by a quadrotor of finite thrust and non-zero mass, a component of the thrust of the quadrotor must counteract gravity, with the remaining being available to support the cable tension. The balance of forces for the i^{th} quadrotor in this example is given by Eq. 10.

$$f_i\mathbf{v}_i + m_i\mathbf{g} - t_i\mathbf{u}_i = 0 \tag{10}$$

The vector form can be decomposed into a system of three equations and four variables, namely t_i, f_i, v_{ix}, v_{iz}.

$$f_i v_{ix} - t_i u_{ix} = 0 \tag{11a}$$
$$f_i v_{iz} + m_i g - t_i u_{iz} = 0 \tag{11b}$$
$$v_{ix}^2 + v_{iz}^2 = 1 \tag{11c}$$

with g being the $\mathbf{g}^T[0,1]^T$. Eliminating v_{ix} and v_{iz} reduces the problem to a single equation linking thrust and tension.

$$t_i^2 - 2u_{iz}m_i g t_i + m_i^2 g^2 - f_i^2 = 0 \tag{12}$$

It is apparent that the maximum achievable tension must occur at the maximum quadrotor thrust, therefore the maximum tension can be mapped from thrust space to tension space by Eq. 13.

$$\bar{t}_i = m_i g u_{iz} + \sqrt{\bar{f}_i^2 + m_i^2 g^2 \left(u_{iz}^2 - 1\right)} \tag{13}$$

Available Wrench Set

The wrench that each cable exerts on the platform can be mapped from tension space to wrench space with the wrench matrix $\mathbf{W}$. The platform is in static equilibrium when $\mathbf{W}\mathbf{t} + \mathbf{w}_e = 0$, where $\mathbf{t} \in \mathcal{T}$ [11, 14].

$$\mathbf{W} = \begin{bmatrix} \mathbf{u}_1 & \ldots & \mathbf{u}_m \\ \mathbf{R}_p\mathbf{b}_1 \times \mathbf{u}_1 & \ldots & \mathbf{R}_p\mathbf{b}_m \times \mathbf{u}_m \end{bmatrix} \tag{14}$$

The wrench space is the set of wrenches that the cables are able to exert on the payload expressed in $\mathcal{F}_0$ as described in Eq. (15), where $\mathbf{w}_i$ is the i^{th} column of the wrench matrix $\mathbf{W}$ and $\Delta t_i =$

$\bar{t}_i - \underline{t}_i$. A wrench $\mathbf{w}$ is inside the available wrench set if and only if it satisfies Eq. (15).

$$\mathcal{W} = \left\{ \mathbf{w} \in \mathbb{R}^d | \mathbf{w} = \sum_{j=1}^{m} \alpha_j \Delta t_j \mathbf{w}_j + \mathbf{W}\underline{\mathbf{t}}, \quad 0 \leq \alpha_j \leq 1 \right\} \quad (15)$$

As the tension space in this example is an orthotope which is necessarily a convex set, the linear mapping of the points bounding the tension space is also a convex set. Therefore the mapping of the vertices of the tension space by the wrench matrix fully and exclusively contains all feasible wrenches. Using the convex hull method described in [15], the achievable wrench set of the system can be found as the convex hull of the set of d-dimensional points $\mathbf{W}_a$.

$$\mathbf{W}_a = \mathbf{W} diag(\Delta \mathbf{t}) \boldsymbol{\alpha} + \mathbf{W}\underline{\mathbf{t}}\, \mathbf{1}_{(1,2^n)} \quad (16)$$

where $\mathbf{1}_{(1,2^n)}$ is a row vector of ones with 2^n columns. In the planar example considered here, the matrix $\boldsymbol{\alpha}$ is the set of all combinations of tension limits bounding the tension space

$$\boldsymbol{\alpha} = \begin{bmatrix} 0 & 0 & 0 & 0 & 1 & 1 & 1 & 1 \\ 0 & 0 & 1 & 1 & 0 & 0 & 1 & 1 \\ 0 & 1 & 0 & 1 & 0 & 1 & 0 & 1 \end{bmatrix} \quad (17)$$

It is apparent that the mapping from tension space vertices to wrench space generates eight wrenches, however the wrench space in Fig. 4 has six vertices only. That is because, due to the redundant nature of the cable system ($m > d$), two mapped tension vertices are internal to the convex set formed by the other six wrenches.

Capacity Margin

The capacity margin γ is an index used to evaluate the robustness of static equilibrium [14,10]. It is defined as the shortest distance from the expected load wrench to the nearest face of the available wrench set. Throughout the entirety of the wrench set determination, the orientation of the quadrotor thrust was held to be arbitrary, constrained solely by its maximum magnitude. This leads to the corollary that the capacity margin can be used to determine the minimum set of external wrenches on the platform that the ACTS can compensate for solely with modifications to the attitude of the quadrotor. As the dynamics of the attitude control of quadrotors are much faster than those of position control, this means that compensating for disturbances with attitude only will provide a more robust system. In this planar case, the attitude of the quadrotor is given by $\mathbf{v}_i = [sin(\phi), cos(\phi)]^T$, such that Eq. (10) is satisfied.

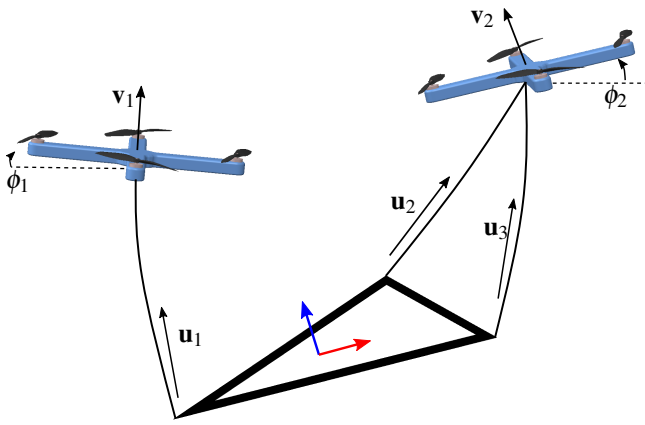

FIGURE 5: DIAGRAM OF PLANAR SYSTEM WITH 2 QUADROTORS AND 3 CABLES

5 CASE STUDIES

Several case studies are provided to demonstrate the computation of the available wrench set. In the first case, a planar ACTS composed of a rigid platforms with two quadrotors and three cables is analyzed, differing from the previous example through a coupling between two dimensions of the tension space, as well as a non-homogenous wrench space. The study is then extended to two 6-DOF spatial systems, the first of which is a redundantly actuated platform with eight quadrotors and eight cables, the other being a system of three quadrotors and six cable such as is used in [8]. All examples use quadrotors with a mass of $0.8kg$ and a maximum thrust of $32N$.

Planar System with 2 Quadrotors and 3 Cables

If the object being transported is large, the moments that can be applied to the platform become of greater importance. Multiple cables attached to a single quadrotor may improve the orientation control of the platform without increasing the number of quadrotors. For the ACTS shown in Fig. (5), the thrust space to tension space mapping of quadrotor 1 to cable 1 can be done using the same methodology as the previous example. The second quadrotor is connected to two cables, and has the equilibrium equation shown in Eq. (18)

$$f_2\mathbf{v}_2 + m_2\mathbf{g} - t_2\mathbf{u}_2 - t_3\mathbf{u}_3 = 0 \quad (18)$$

To determine the tensions in the two cables, there are 5 variables $(f_2, t_2, t_3, v_{2x}, v_{2z})$. An additional equation is found as $\mathbf{v}_2$ is a unit

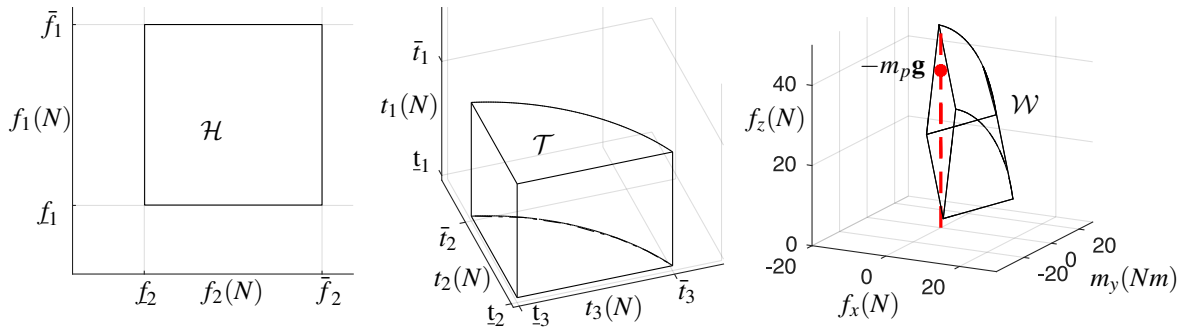

A) THRUST SPACE B) TENSION SPACE C) WRENCH SPACE

FIGURE 6: THRUST, TENSION, AND WRENCH SPACES OF PLANAR ACTS WITH 2 QUADROTORS AND 3 CABLES

vector, resulting in as system of 3 equations.

$$f_2 v_{2x} - t_2 u_{2x} - t_3 u_{3x} = 0 \tag{19a}$$
$$f_2 v_{2z} - t_2 u_{2z} - t_3 u_{3z} + m_2 g = 0 \tag{19b}$$
$$v_{2x}^2 + v_{2z}^2 = 1 \tag{19c}$$

This set of equations can be reduced to an equation relating the thrust of the quadrotor to the magnitude of the two cable tensions.

$$t_2^2 + t_3^2 + 2t_2 t_3 \left(\mathbf{u}_2^T \mathbf{u}_3\right) - 2m_2 g(t_2 u_{2z} + t_3 u_{3z}) + m_2^2 g^2 - f_2^2 = 0 \tag{20}$$

By writing Eq. (20) to solve for t_2 as $t_2 = h_2(t_3, f_2)$ and likewise $t_3 = h_3(t_2, f_2)$ the cable tension space can be formulated as

$$\mathcal{T} = \mathbf{t} \in \mathbb{R}^3 \begin{cases} \underline{t}_1 \le t_1 \le \bar{t}_1 \\ \underline{t}_2 \le t_2 \le h_2(t_3, \bar{f}_2) \\ \underline{t}_3 \le t_3 \le h_3(t_2, \bar{f}_2) \end{cases} \tag{21}$$

The main difference in computing the available wrench set for this system is the $\boldsymbol{\alpha}$ matrix used in Eq. (16). Appendix A proves that, given the sufficient conditions of all cables projecting along the positive $\mathbf{z}_0$ axis, and the angle between cables j and k being less than $\frac{\pi}{2} rad$, the function $h_j(t_k, \bar{f}_i)$ is convex over the domain $\underline{t}_k \le t_k \le \bar{t}_k$. This property guarantees that the mapping of any set of points in the tension space produces a convex set exclusively containing feasible wrenches. In Fig. (6b), six vertices are clearly identifiable, however mapping only these points will result in an over conservative set of available wrenches. To approximate the full wrench set, the arc between $\bar{t}_2$ and $\bar{t}_3$ is divided into $p+1$ segments. The combination matrix of the tension span of the second and third cables is denoted as $\boldsymbol{\alpha}_{23}$.

$$\boldsymbol{\alpha} = \begin{bmatrix} \mathbf{0}_{(1,3+p)} & \mathbf{1}_{(1,3+p)} \\ \boldsymbol{\alpha}_{23} & \boldsymbol{\alpha}_{23} \end{bmatrix} \tag{22}$$

The $\boldsymbol{\alpha}_{23}$ matrix includes the three vertices of the t_2, t_3 plane, and a set of vertices evaluated at interpolation points $t_{3,k} = h_3(t_{2,k}, \bar{f}_2)$ for all interpolation points $k \in \mathbb{Z} \mid 1 \le k \le p$. The full $\boldsymbol{\alpha}_{23}$ matrix is shown in Eq. (23).

$$\boldsymbol{\alpha}_{23} = \begin{bmatrix} 0 & 1 & 0 & \frac{k}{p+1} & \cdots & \frac{p}{p+1} \\ 0 & 0 & 1 & \dfrac{h_3(\frac{k\Delta t_2}{p+1} + \underline{t}_2) - \underline{t}_3}{\Delta t_3} & \cdots & \dfrac{h_3(\frac{p\Delta t_2}{p+1} + \underline{t}_2) - \underline{t}_3}{\Delta t_3} \end{bmatrix} \tag{23}$$

As the available wrench set of this robot is $\mathbf{w} \in [f_x, f_z, m_y]$, it must be homogenized to allow for a calculation of the capacity margin. In [10], the capacity margin is homogenized by dividing the moment by the radius of gyration $r_g = \sqrt{I/A}$ of the platform, where A is the area of the platform and I is the second area moment of inertia. If $\mathbf{W}_a$ is the matrix whose columns form a set of points bounding the convex wrench space, the homogenized wrench space boundary is given by Eq. (24).

$$\mathbf{W}_h = \begin{bmatrix} \mathbb{I}_2 & 0 \\ 0 & \dfrac{1}{r_g} \end{bmatrix} \mathbf{W}_a \tag{24}$$

where $\mathbb{I}_2$ is an identity matrix of rank 2. In this case study the system parameters are defined as: pose $\mathbf{p} = [0, 0, pi/6]$, platform mass $m_p = 4kg$, platform dimensions $\mathbf{b}_1 = [-0.75, -0.25]^T, \mathbf{b}_2 = [0.5, 0.5]^T, \mathbf{b}_3 = [1.0, -0.25]^T$, cables of 0.75m in length, and $\mathbf{u}_1 = [0, 0, 1]^T$. Fig. (6c) shows the available wrench set, with the dotted line indicating the line along f_z passing through $f_x = 0, m_y = 0$. The capacity margin of the ACTS in this configuration is 0.3N, so this configuration is on the border of equilibrium. It is noteworthy that solely reducing m_p here does little to change γ, but that γ increases significantly with a combination of $\mathbf{w}_e = [0, 0, -m_y]$ and decreased m_p. The attitudes ϕ_1 and ϕ_2 of the quadrotors are chosen such that for the point in tension space $\mathbf{t} = \mathbf{W}^{-1}(m_p\mathbf{g} - \mathbf{w}_e)$, Eq. (10) is satisfied for the first quadrotor, and Eq. (18) is satisfied for the second quadrotor.

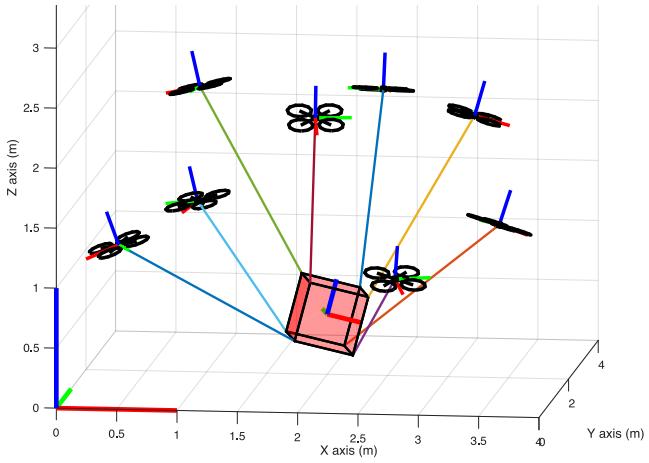

FIGURE 7: ACTS WITH 8 QUADROTORS AND 8 CABLES

Spatial System with 8 Quadrotors and 8 Cables

In this case, the platform is desired to have a controllable orientation without holonomic constraints on the twist. The ACTS, shown in Fig. (7) has a cubic moving platform with side lengths of $0.5m$, mass $m_p = 4kg$, and orientation of $[\frac{\pi}{12}, \frac{\pi}{12}, 0]rad$. It is manipulated by eight quadrotors so that all twists are achievable with two degrees of actuation redundancy in non-singular states. A configuration has been chose to avoid singularities for the evaluation of the available wrench set. The vector $\mathbf{u}_i$ of the cables connected to the lower vertices of the platform are rotated by $\frac{-\pi}{6}rad$ from the direction of $\mathbf{b}_i$ about $\mathbf{z}_0$, and the given an elevation of $\frac{\pi}{6}rad$ from the xy plane. The top vertices cables are rotated in the opposite direction by $\frac{\pi}{6}rad$ from $\mathbf{b}_i$ about $\mathbf{z}_0$, and then elevated by $\frac{\pi}{3}rad$.

In this case, the thrust space is computed for each quadrotor as in the previous section, resulting in a 8-orthotope. The tension space is likewise calculated to result in an 8-orthotope by extending Eq. (11a) to a 3rd dimension, adding the equation $f_i v_{iy} - t_i u_{iy} = 0$. The result is the same as in the planar system, with the thrust space to tension space mapping being described by Eq. (13). The vertices of the thrust and tension spaces are combinations of maximum and minimum thrust and tension values in Table (1).

Mapping the vertices of the tension space orthotope to task space results in a convex 6-zonotope [12, 15] bounding the available wrench set of the ACTS. Fig. (8) shows the evaluation of the available wrench set at zero moment (8a) and at $f = -m_p\mathbf{g}$ (8b). From this, it is seen that the system can exert a force wrench between 10N and 120N along $\mathbf{z}_0$, and forces between -20N and 20N laterally, with the largest lateral wrench range occuring when the vertical force is around 60N. This ACTS has little ability to withstand positive moments about $\mathbf{z}_0$ limiting the capacity margin to $\gamma = 6.5N$. This ACTS configuration would be useful in situations

TABLE 1: THRUST SPACE AND CABLE TENSION SPACE LIMITS FOR 8 QUADROTOR, 8 CABLE CASE STUDY.

Quadrotor	$\underline{f}(N)$	$\bar{f}(N)$	Cable	$\underline{t}(N)$	$\bar{t}(N)$
1	8.7	32.0	1	1.0	25.0
2	8.4	32.0	2	1.0	27.4
3	8.7	32.0	3	1.0	25.0
4	8.4	32.0	4	1.0	27.4
5	8.7	32.0	5	1.0	25.0
6	8.4	32.0	6	1.0	27.4
7	8.7	32.0	7	1.0	25.0
8	8.4	32.0	8	1.0	27.4

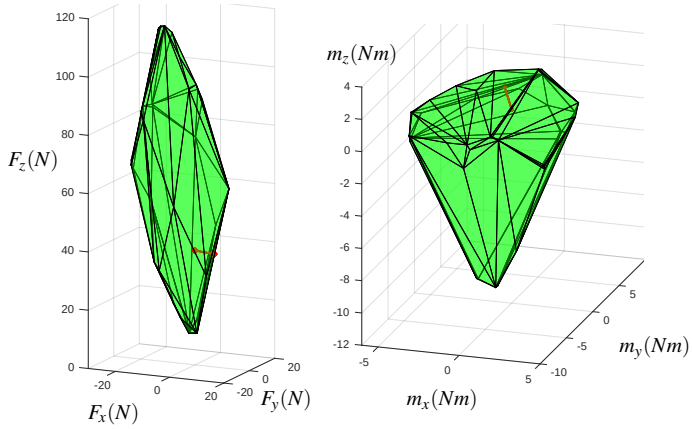

FIGURE 8: ACHIEVABLE WRENCH SPACE OF 8 QUADROTOR, 8 CABLE ACTS EVALUATED AT $MOMENT = [0,0,0]Nm$ (LEFT) AND $FORCE = -m_p\mathbf{g}\,N$ (RIGHT)

that required (primarily vertical) movements, as well as roll and pitch capabilities, but without strict yaw requirements.

While the wrench feasibility can be quantified using the capacity margin after normalizing $\mathbf{W}_a$ by Eq. (25), the configuration of this particular ACTS does not lend itself well toward numerical optimization, as the set of variables (the altitude and azimuth of each cable) is 16 dimensional. Intuitive configurations avoiding common singularities can however, be evaluated for their robustness.

$$\mathbf{W}_h = \begin{bmatrix} \mathbb{I}_3 & 0 \\ 0 & \frac{\mathbb{I}_3}{r_g} \end{bmatrix} \mathbf{W}_a \tag{25}$$

The attitude of the quadrotors must be controlled so as to chose $\mathbf{v}_i$ satisfying $f_i\mathbf{v}_i + m_i\mathbf{g} - t_i\mathbf{u}_i = 0$. As the system is redundant, tension distribution algorithms may be used to specify the desired

tensions, and therefor attitudes. In this case, using the Moore-Pensrose pseudo-inverse of $\mathbf{W}$ finds the least norm cable tensions, and vector $\boldsymbol{\lambda}$ is chosen so that $\mathbf{t}$ is within $\mathcal{T}$. The vector $\mathbf{v}_i$ may be found for all quadrotors using Eq. (10).

$$\mathbf{t} = \mathbf{W}^{\dagger}(\mathbf{w_e} - m_p\mathbf{g}) + \mathbf{N}\boldsymbol{\lambda}, \text{ where } \mathbf{N} = null(\mathbf{W}) \tag{26}$$

The rotation matrix of each quadrotor is under-constrained by 1-DOF, as the rotation of the i^{th} quadrotor around $\mathbf{v}_i$ has no affect on the system equilibrium [16], and any rotation matrix of the under-constrained quadrotor may be chosen so long as the equation $\mathbf{R}_i[0,0,1]^T = \mathbf{v}_i$ is satisfied.

Spatial System with 3 Quadrotors and 6 Cables

The Flycrane ACTS has been studied for motion planning in [8], and is composed of three quadrotors and six cables. A benefit of this design is the ability to generate six independent wrenches using only three quadrotors. It also has the advantage of being significantly easier to optimize, with a three dimensional configuration space compared to the 16 dimensional configuration space in the previous case.

The ACTS in this case is displayed in Fig. (9). platform orientation is $[\frac{\pi}{12}, \frac{\pi}{12}, 0] rad$ and $m_p = 4kg$. The platform is parameterized as $\mathbf{b}_i = 0.5\left[cos\left(\frac{2\pi i}{6}\right), sin\left(\frac{2\pi i}{6}\right), 0\right] m, i \in \mathbb{Z}, 1 \leq i \leq 6$. The cable pairs have lengths of $L_{1,2} = 0.35m$, $L_{3,4} = 0.70m$, and $L_{5,6} = 1.40m$. Each quadrotor is at an inclination of $\frac{\pi}{4} rad$ from the $\mathbf{z}_p$ axis.

The 3-orthotope thrust space is mapped to the 6-dimensional cable tension space, with the tension in each pair of cables (j and k) being related to the thrust of a single quadrotor (i) through Eq. (27).

$$f_i\mathbf{v}_i + m_i\mathbf{g} - t_j\mathbf{u}_j - t_k\mathbf{u}_k = 0 \tag{27}$$

To determine the tensions in the two cables, there are 6 variables $(t_j, t_k, f_i, v_{ix}, v_{iy}, v_{iz})$. An additional equation is found as $\mathbf{v}_i$ is a unit vector, resulting in 4 equations with 6 unknowns. This reduces to the same result as seen in Eq. (20), generalized in Eq. (28) for cables j and k.

$$t_j^2 + t_k^2 + 2t_jt_k\left(\mathbf{u}_j^T\mathbf{u}_k\right) - 2m_ig(t_ju_{jz} + t_ku_{kz}) + m_i^2g^2 - f_i^2 = 0 \tag{28}$$

Each of the three orthogonal 2-dimensional tension space components, which are all composed of straight lines along the lower bound tensions, and the upper bound tension is described by an analytic function h, where $t_j = h_j(t_k, \bar{f}_i)$, creating a 6 dimensional solid composed of a combination of flat and curved surfaces. It is seen that for longer cables ($\mathbf{u}_j^T\mathbf{u}_k \approx 1$), the upper bound of the curve approaches a straight line joining the vertices $\left(\underline{t}_j, h_k(\underline{t}_j, \bar{f}_i)\right)$ and $\left(h_j(\underline{t}_k, \bar{f}_i), \underline{t}_k\right)$. As the number of interpolation points p along the curve $t_j = h_j(t_k, \bar{f}_i)$ increases, the size of the convex set of points increases by the cube of the number of points $(3+p)^3$. Short cables relative to the baseline separating the cables increases the curvature of the maximum tension curve, increasing the importance of interpolations. The vertices of the thrust space and the cable tension space are shown in Table (2). In the same manner as is done for the planar system with two quadrotors and three cables, the available wrench space of this ACTS can be mapped through interpolation along the convex curved surfaces. The combination matrix $\boldsymbol{\alpha}$ is built as all combinations of the columns of $\boldsymbol{\alpha}_{jk}$, derived as in Eq. (23), and arranged as shown in Eq. (29)

$$\boldsymbol{\alpha} = comb\left(\begin{bmatrix}\boldsymbol{\alpha}_{12}\\ \boldsymbol{\alpha}_{34}\\ \boldsymbol{\alpha}_{56}\end{bmatrix}\right) \tag{29}$$

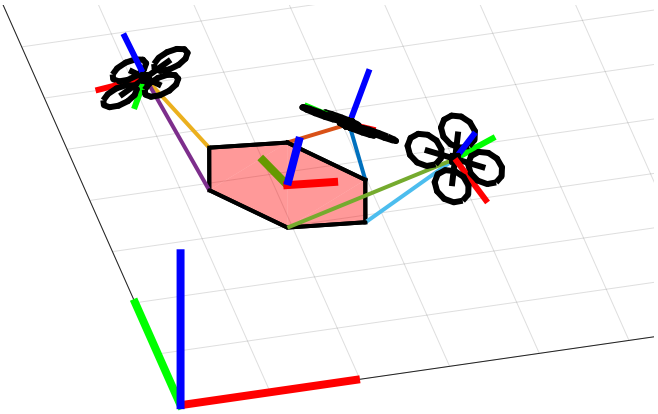

FIGURE 9: EXAMPLE OF FLYCRANE ACTS

TABLE 2: THRUST SPACE AND TENSION SPACE LIMITS FOR FLYCRANE CASE STUDY

Quadrotor	$\underline{f}(N)$	$\bar{f}(N)$	Cable	$\underline{t}(N)$	$\bar{t}(N)$
1	8.6	32.0	1	1.0	27.6
			2	1.0	28.8
2	9.5	32.0	3	1.0	24.4
			4	1.0	24.9
3	9.3	32.0	5	1.0	25.5
			6	1.0	25.0

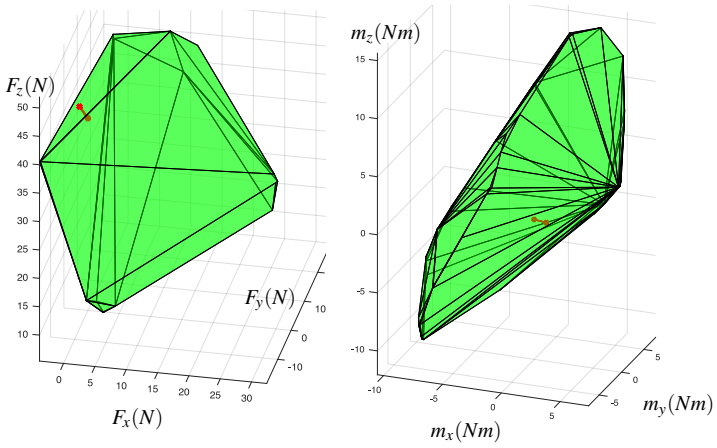

FIGURE 10: ACHIEVABLE WRENCH SPACE OF FLY-CRANE ACTS EVALUATED AT $MOMENT = [0,0,0]Nm$ (LEFT) AND $FORCE = -m_p\mathbf{g}N$ (RIGHT)

The available wrench set of the ACTS is shown in Fig. (10). The ACTS in this configuration can apply a peak force of 50N along $\mathbf{z}_0$, and a peak force of 30N in the positive $\mathbf{x}_0$ direction, however it has can only exert a force of 2N along the negative $\mathbf{x}_0$ axis. It is able to exert moments from -10 Nm to 15 Nm about $\mathbf{z}_0$, but much less around $\mathbf{x}_0$ and $\mathbf{y}_0$.

6 CONCLUSIONS AND FUTURE WORK

In this paper, it is shown how the available wrench set of the payload of an aerial cable towed system (ACTS) can be calculated. This method is adaptable to systems where two cables are coupled due to sharing the actuation of a single quadrotor. It is proven that the relationship between tensions in such a coupled system is necessarily convex given certain operational and design conditions, showing that the available wrench set obtained from a mapping of the tension space is guaranteed to be conservative throughout the wrench space.

From a practical point of view, this has applications in the optimal design and motion planning of ACTS with the objective of increasing the ability to resist external wrenches acting on the moving platform. As the available wrench set is determined through a mapping of the full achievable tension space of the system, it can be seen that the position of the platform and the configuration of the system can be maintained while the external wrench is within the bounds of the available wrench set through changes in attitude of the quadrotor, requiring no change in the quadrotors positions. The higher dynamic response of attitude control compared to position control may lead to improvements in response time to system disturbances.

Future work will include experimental validation of the available wrench set calculations by testing the reaction of ACTSs to wrenches lying inside and outside of the available wrench space. The analysis will then be extended to dynamic systems, and the implementation of the available wrench set calculation for generating trajectories optimized for the robustness of equilibrium of the system will be performed.

NOMENCLATURE

TABLE 3: LIST OF NOMENCLATURE, DIVIDED INTO GENERAL, QUADROTOR, AND CDPR CLASSES

Symbol	Description
$\mathcal{F}_0$	Inertial reference frame
$\mathcal{H}$	Thrust space of ACTS
$\mathcal{T}$	Tension space of ACTS
$\mathcal{W}$	Wrench space of ACTS
d	Dimension of task space
m	Number of cables
n	Number of quadrotors
$\mathbf{x}_0, \mathbf{y}_0, \mathbf{z}_0$	x, y, and z unit vectors of $\mathcal{F}_0$
$\mathbf{g}$	Gravitational vector $[0,0,-9.81]^T \quad ms^{-2}$
g	Scalar gravity $\mathbf{g}^T\mathbf{z}_0$
$\mathcal{F}_i$	Reference frame of quadrotor i
A_i	Attachment point of cables to quadrotor i (in $\mathcal{F}_0$)
C_F, C_M	Coefficients of thrust and drag of propellors
$\underline{f}_i, \bar{f}_i$	Min. and max. allowable thrust of quadrotor i
m_i	Mass of quadrotor i
$\mathbf{R}_i$	Rotation matrix of $\mathcal{F}_i$ with respect to $\mathcal{F}_0$
$\mathbf{v}_i$	Unit vector normal to propellors of quadrotor i
$\mathbf{x}_i$	Position of quadrotor i expressed in $\mathcal{F}_0$
ω_i	Angular rotation of propellor i
$\mathcal{F}_p$	Reference frame of platform
$\boldsymbol{\alpha}$	Combination matrix
$\mathbf{b}_i$	Vector from $\mathbf{p}$ to cable i connection point (in $\mathcal{F}_p$)
B_i	Point where cable i connect to platform (in $\mathcal{F}_0$)
l_i	Length of cable i
m_p	Mass of platform
$\mathbf{p}$	Position of platform center of mass expressed in $\mathcal{F}_0$
${}^0\mathbf{R}_p$	Rotation matrix of $\mathcal{F}_p$ with respect to $\mathcal{F}_0$
$\mathbf{t}_i$	Force vector exerted by cable i at point B_i
$\mathbf{t}$	Vector of cable tensions $[t_1, \ldots, t_m]^T$
$\underline{t}_i, \bar{t}_i$	Min. and max. allowable tensions in cable i
$\mathbf{u}_i$	Unit vector from B_i to A_i
$\mathbf{W}$	Wrench matrix of platform
$\mathbf{W}_a$	Set of available wrench vectors of the ACTS
$\mathbf{w}_e$	External wrench acting on platform

REFERENCES

[1] Kumar, V., and Michael, N., 2012. "Opportunities and challenges with autonomous micro aerial vehicles". *The International Journal of Robotics Research,* ***31***(11), August, pp. 1279–1291.

[2] Tagliabue, A., Kamel, M., Verling, S., Siegwart, R., and Nieto, J., 2017. "Collaborative transportation using mavs via passive force control". In Proceedings of the International Conference on Robotics and Automation, IEEE.

[3] Tognon, M., and Franchi, A., 2017. "Dynamics, control, and estimation for aerial robots tethered by cables or bars". In IEEE Transaction on Robotics, Vol. 33, IEEE.

[4] Lee, T., Leoky, M., and McClamroch, N. H., 2010. "Geometric tracking control of a quadrotor uav on se(3)". In Proceedings of the 49th IEEE Conference on Decision and Control, IEEE, ed., IEEE.

[5] Sreenath, K., and Kumar, V., 2013. "Dynamics, control and planning for cooperative manipulation of payloads suspended by cables from multiple quadrotor robots". In Robotics: Science and Systems.

[6] Masone, C., Bülthoff, H., and Stegagno, P., 2016. "Cooperative transportation of a payload using quadrotors: a reconfigurable cable-driven parallel robot". In International Conference on Intelligent Robots and Systems, IEEE.

[7] Alothman, Y., Guo, M., and Gu, D., 2017. "Using iterative lqr to control two quadrotors transporting a cable-suspended load". *International Federation of Automatic Control IFAC-papers online,* ***50***, July, pp. 4324–4329.

[8] Manubens, M., Devaurs, D., Ros, L., and Cortes, J., 2013. "Motion planning for 6-d manipulation with aerial towed-cable systems.". In Robotics: Science and Systems, p. 8.

[9] Bosscher, P., Riechel, A., and Ebert-Uphoff, I., 2006. "Wrench-feasible workspace generation for cable-driven robots". In IEEE Transaction on Robotics, Vol. 22, IEEE.

[10] Gagliardini, L., Caro, S., Gouttefarde, M., and Girin, A., 2016. "Discrete reconfiguration planning for cable-driven parallel robots". *Mechanism and Machine Theory,* ***100***, pp. 313–337.

[11] Azizian, K., and Cardou, P., 2013. "The dimensional synthesis of spatial cable-driven parallel mechanisms". *Journal of Mechanisms and Robotics,* ***5***(4), November.

[12] Gosselin, C., 2014. "Cable-driven parallel mechanisms: state of the art and perspectives". *Bulletin of the Japan Society of Mechanical Engineers,* ***1***(1).

[13] Michael, N., Fink, J., and Kumar, V., 2011. "Cooperative manipulation and transportation with aerial robots". *Autonomous Robots,* ***30***, January.

[14] Cruz Ruiz, A. L., Caro, S., Cardou, P., and Guay, F., 2015. "Arachnis: Analysis of robots actuated by cables with handy and neat interface software". *Mechanisms and Machine Science,* ***32***, pp. 293–305.

[15] Bouchard, S., Gosselin, C., and Moore, B., 2010. "On the ability of a cable-driven robot to generate a prescibed set of wrenches". *ASME Journal of Mechanisms and Robotics,* ***2***(1).

[16] Lee, T., Sreenath, K., and Kumar, V., 2013. "Geometric control of cooperating multiple quadrotor uavs with a suspended payload". In Proceedings of the 52nd IEEE Conference on Decision and Control, IEEE.

Appendix A: Proof of Convex Tension Space

This appendix proves that the function relating the maximum tensions of two cables i, j connected to quadrotor Q forms a convex tension space. Equation 20 can be rewritten as

$$\bar{t}_i^2 + \bar{t}_j^2 + k_1\bar{t}_i\bar{t}_j + k_2\bar{t}_i + k_3\bar{t}_j + c \quad | \quad 0 < \underline{t} \leq \bar{t} \leq \bar{t}_{max} \tag{30}$$

where $k_1 = \mathbf{u}_i^T\mathbf{u}_j$, $k_2 = -2m_Q g u_{iz}$, $k_3 = -2m_Q g u_{jz}$, and $c = m_Q^2 g^2 - \bar{f}_Q^2$

The maximum tension of cable j, $\bar{t}_j$ relates to $\bar{t}_i$ through the function $t_j = h_j(t_i, f_Q)$, with $\bar{t}_j = h_j\left(\underline{t}_i, \bar{f}_Q\right)$. The function is convex if, over the span of allowable tensions, it can be shown that $\frac{d\bar{t}_j}{dt_i} \leq 0$ and that $\frac{d^2\bar{t}_j}{dt_i^2} \leq 0$ (sufficient conditions, not necessary). Using implicit differentiation, it can be found that the derivative of $\bar{t}_j$ with respect to t_i is

$$\frac{d\bar{t}_j}{dt_i} = -\frac{2\bar{t}_j + k_1 t_i + k_2}{2t_i + k_1\bar{t}_j + k_3} \tag{31}$$

Assumption number 4 requires that u_z be positive for all cables, therefore k_2 and k_3 are both positive. Applying a simple design rule $\sqrt{l_i^2 + l_j^2} \geq \|B_j - B_i\|$ forces $0 \leq k_1 \leq 1$. With strictly positive tensions, and $k_1, k_2, k_3 \geq 0$, $\frac{d\bar{t}_j}{dt_i}$ is strictly negative.

By setting $\frac{d\bar{t}_j}{dt_i} = -\frac{g}{h}$, the quotient rule and the law of implicit differentiation can be used to solve the second derivative.

$$\frac{d^2\bar{t}_j}{dt_i^2} = -\frac{g\left(\frac{g}{h} - k_1\right) + h}{h^2} < 0 \tag{32}$$

It is therefore shown that within the domain of t_i, given that all cable vectors have a positive projection along the z axis, and that the angle between two cables connected a quadrotor is acute, the tension space is a convex shape.